RSC Advances

PAPER

View Article Online
View Journal | View Issue

Cite this: *RSC Adv.*, 2023, **13**, 29489

Role of the solvent polarity on the optical and electronic characteristics of 1-iodoadamantane

Aravindhan R.,[a] Jianping Hu*[b] and M. Ummal Momeen *[a]

Received 4th August 2023
Accepted 25th September 2023

DOI: 10.1039/d3ra05297d

rsc.li/rsc-advances

The natural absorbance caused by the chromophore and chemical behavior of 1-iodoadamantane is highly influenced by the polarity of different solvent environments. This gives rise to the solvatochromatic shifts in the optical absorption and electronic structure and the experimentally measured UV-vis absorption spectra show significant solvatochromic shifts with respect to the solvent polarity. The absorption shift for both σ to σ*and n to σ* electronic transitions are more dominant in polar solvents than in nonpolar solvents. To obtain a better understanding of the impact of solvent polarity on the 1-iodoadamantane at the molecular level, computational calculations were carried out through implicit solvation. According to this, changes in the HOMO and LUMO energies and electron density distributions of various solvent continuums demonstrate the influence of solvent polarity on the HOMO and LUMO energy levels of the chemical system. This also shows an increment in the HOMO–LUMO gap with respect to the polarity of the solvent.

Introduction

The impact of carbon-based materials in modern technology thrives the fascination towards carbon-based materials in the contemporary situation. Diamondoids are found to be the one among this intriguing group. Small saturated hydrocarbon molecules with cyclohexane rings fused in the form of diamond clusters are called diamondoids. Diamondoids are known for the three-dimensional array of diamond lattice, which combines many beneficial properties of inorganic materials and hydrocarbon molecules at the nanoscale. This makes diamondoids exceptional in terms of structural and electronic properties with high thermal stability.[1,2] Adamantane is found to be the simplest diamondoid in nature, which is composed of cyclohexane rings in the chair conformation. It contains a single aliphatic tetrahedral carbon cage with a molecular formula of $C_{10}H_{16}$.[3–5]

Functionalized adamantane derivatives are of great interest in many applications ranging from materials chemistry to composite materials and 3D porous networks.[6,7] The inclusion of halogens and functional groups, such as amines and esters, on the tertiary carbons is increasingly in demand for the materials technologies.[4,5] The possibility of tuning the band gap in lower dimensional materials is attractive in nanoscale research. Rigid strain-free ring systems of diamondoids are also offering this luxury. Adamantane functionalization is more eclectic than functionalization in polymantanes for the existence of two kinds of C–H bonds. This is found to be an effective choice for tuning the electronic properties of lower diamondoids when compared to the other substituted diamondoids from many perspectives.[8] In this study, the monosubstituted derivative of adamantane with iodine in the bridgehead tertiary carbon atom, namely, 1-iodoadamantane (IAD) is considered. An enduring interest in the solvent effects on the optical properties of the solute paved the way for our findings.[9] It is noticed that the electronic spectra of the compound in the gas phase was completely different in comparison with the solvation. Our study demonstrates significant solvent effects on the electronic absorption of IAD through the experimental UV-vis spectra. Also, computationally noticeable changes are obtained from the HOMO and LUMO energies, and electronic density distribution of the IAD molecule in different solvent media.

Computational methods

Complex excited state geometry and nearly degenerate excited states of halogen-substituted adamantane encounter challenging issues for the theoretical calculations of 1-iodoadamantane (Fig. 1). In many cases, lowest-lying excited states are one of the reasons for the inaccurate predictions of potential energy surfaces in quantum chemical calculations.[10] To overcome this drawback, the employment of high electron correlation methods and large zeta basis sets is found to be an effective option. The coupled cluster singles and doubles (CCSD) method can account for high electron correlation.[11,12]

The framework of coupled clusters provides an infinite perturbation theory in the form of an exponential cluster

[a]*Magnetic Instrumentation and Applied Optics Laboratory, Department of Physics, School of Advanced Sciences, Vellore Institute of Technology, Vellore-632014, India. E-mail: ummalmomeen@gmail.com*

[b]*The College of Nuclear Technology and Automation Engineering, Chengdu University of Technology, Chengdu, P. R. China. E-mail: profjianpinghu@hotmail.com*

operator for a better description of electronic wavefunctions.[13,14] The equation of motion-coupled cluster singles and doubles (EOM-CCSD) is a form of coupled cluster theory introduced for the robust description of the excited states. EOM-CCSD is preferred to attain the exact excited state and potential energy surfaces for bond-breaking conditions.[15,16] In the case of EOM-CCSD, the excited state wavefunctions are attained using an excitation operator.[17–19] To achieve exact excited state energies, all the calculations were carried out with EOM-CCSD high electron correlated methods in Gaussian 16 and for visualization, Gauss View 6 was used.[20,21] Choosing a proper basis set is tedious for the molecules consisting of heavy atoms such as iodine to attain better accuracy. Smaller basis sets, which are used for providing the correct description of the electronic structure of molecules in the self-consistent field (SCF) are majorly not adequate to account for both intra- and interatomic distance in equal proportion. Due to the high atomic energies of iodine, small basis sets are not suitable for providing the complete description of the molecular system.[22] As such, for the accurate description of IAD, we carried out our calculations with the set of effective core potential (ECP), and all-electron basis sets were named LanL2DZ and MidiX.[23–27]

Solvation effects are computationally included by means of the solvent model density (SMD) solvation model developed by Marenich *et al.* through the self-consistent reaction field (SCRF) formalism.[28,29] SMD model is applicable to all charged and uncharged solutes. Further, dielectric constant, refractive index, bulk surface tension, acidity, and basicity are taken as key descriptors for the solvents. In the SMD model, the charge density of the solute induces the polarization in the solvent dielectric medium and the self-consistent interaction between the charge density of the solute and the polarization field of the solvent continuum confers the free energy of solvation.[28] In solvation, a standard-state free energy of transfer from the gas phase to the condensed phase are partitioned and shown as

$$\Delta G^{\circ}_{S} = \Delta G_{ENP} + G_{CDS} + \Delta G^{\circ}_{Con} \quad (1)$$

ΔG_{ENP} represents electronic nuclear polarization components of free energy of the solvation and G_{CDS} emphasize change in the free energy with respect to the solvent cavitation (C), changes in the dispersion energy (D) and local solvent structure (S), ΔG°_{Con} represents the concentration change between the gaseous state and the liquid state.[28] Solvents in our study were selected based on the fundamental descriptors, namely dielectric constant (ε), relative polarity, and Kamlet–Taft solvatochromatic parameters (α, β, π^*).[28,30–34]

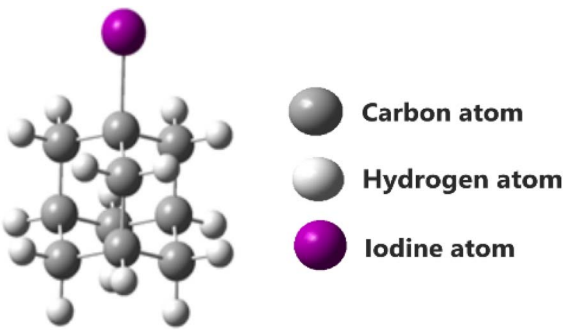

Fig. 1 1-Iodoadamantane molecule.

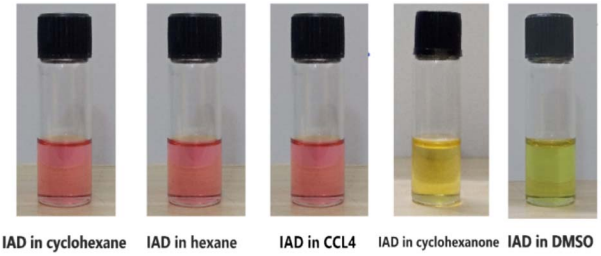

Fig. 2 The significant color change is shown for the IAD solutions formed with the solvents.

Experimental procedures

To measure the UV-vis absorption spectra, homogenous solutions of 1-iodoadamantane were prepared in both nonpolar (cyclohexane, hexane, and carbon tetrachloride (CCL4)) and polar solvents (cyclohexanone and dimethyl sulfoxide (DMSO)).

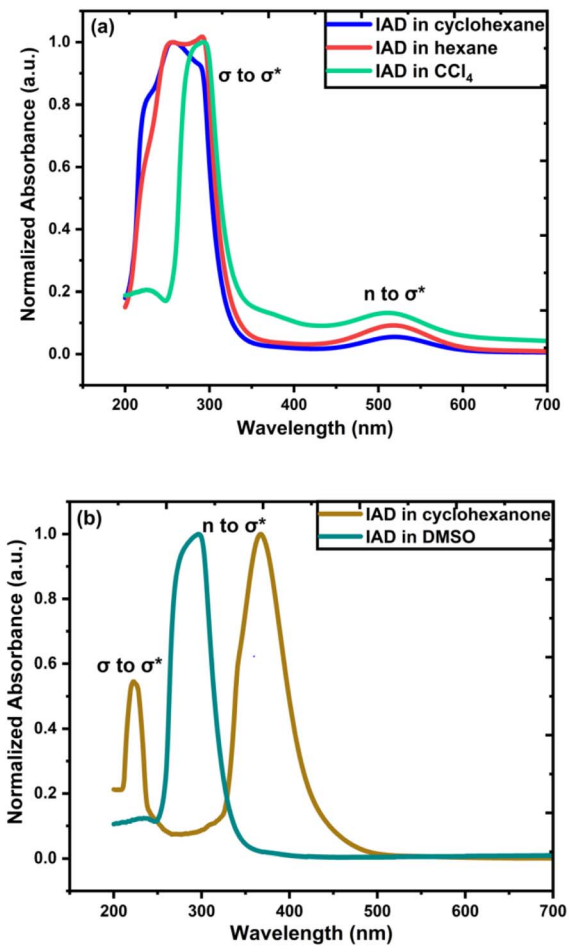

Fig. 3 (a) Effects of solvent on experimental UV-vis spectra for IAD in nonpolar solvents, and (b) solvent effects on experimental UV-vis for IAD in polar solvents.

Table 1 Comparison of the maximum absorption wavelengths between the experimental measurements and computed results (EOM-CCSD)

Solvents	Experimental	Computed
Cyclohexane	256 nm, 515 nm	336 nm, 526 nm
Hexane	290 nm, 517 nm	345 nm, 548 nm
CCL4	293 nm, 519 nm	330 nm, 509 nm
Cyclohexanone	223 nm, 366 nm	194 nm, 296 nm
DMSO	297 nm	194 nm, 291 nm

Solvents with different dielectric constants for this study were chosen and classified as polar and nonpolar solvents with respect to the polarity.[35–37] Homogenous IAD solutions were prepared in 10 mg ml^{-1}, 20 mg ml^{-1}, 50 mg ml^{-1}, 80 mg ml^{-1}, and 100 mg ml^{-1} concentrations in both polar and nonpolar solvents. Solvent effects on the UV-vis spectra were measured using the Jasco V-670 spectrophotometer at a concentration of 10 mg ml^{-1}, which is shown in Fig. 3. The experimental results were compared with the computed absorption spectra, as shown in Fig. 4. The solvent concentration effects of the IAD in various solvents are also shown in Fig. 4.

Results and discussion

The experimental and theoretical results of this study demonstrated the crucial solvent effect on the photophysical and electronic properties of IAD. This causes a significant color change between the polar and non-polar solvents, as shown in Fig. 2.

Solvent effects on absorption spectra

Absorption spectra of IAD have two possible absorption bands.[38,39] The absorption band in the vacuum UV region corresponds to the σ to σ* transition and the absorption band at 450 nm corresponds to the n to σ* electronic transition. In the solvation phase, all nonpolar solvents exhibit red shift for absorption due to σ to σ* transition and n to σ* transition by the higher stabilization of the excited state (Fig. 3). In polar solvents, an increase in the solvent polarity makes the ground state more stabilized than the excited state and causes a blue shift for both σ to σ* transition and n to σ* transition.[36–41] Large dipole moments of polar solvents cause significant stabilization of the iodine atom.

Solvent effects are more significant in polar solvents due to the change in the charge density of the solute caused by the solvent, which alters the electronic distribution of IAD and results in the solvatochromatic shifts.[33,35] These changes are less in the nonpolar solvents due to the small dielectric constant possessed by the solvents. The strength of the electronic transitions is illustrated by the oscillator strength, which allowed us to clearly examine a band with a lower absorption intensity. A less intense peak in the nonpolar solvents approximately at 500 nm was identified computationally by the values of oscillator strength for the electronic transition. In addition to the solvent effects, absorption of IAD in different solvents also undergoes significant variations with respect to the concentration of IAD irrespective of the polarity of solvents. The noticeable difference obtained between the experimentally measured and computed absorption, as shown in Table 1 and Fig. 4, is due

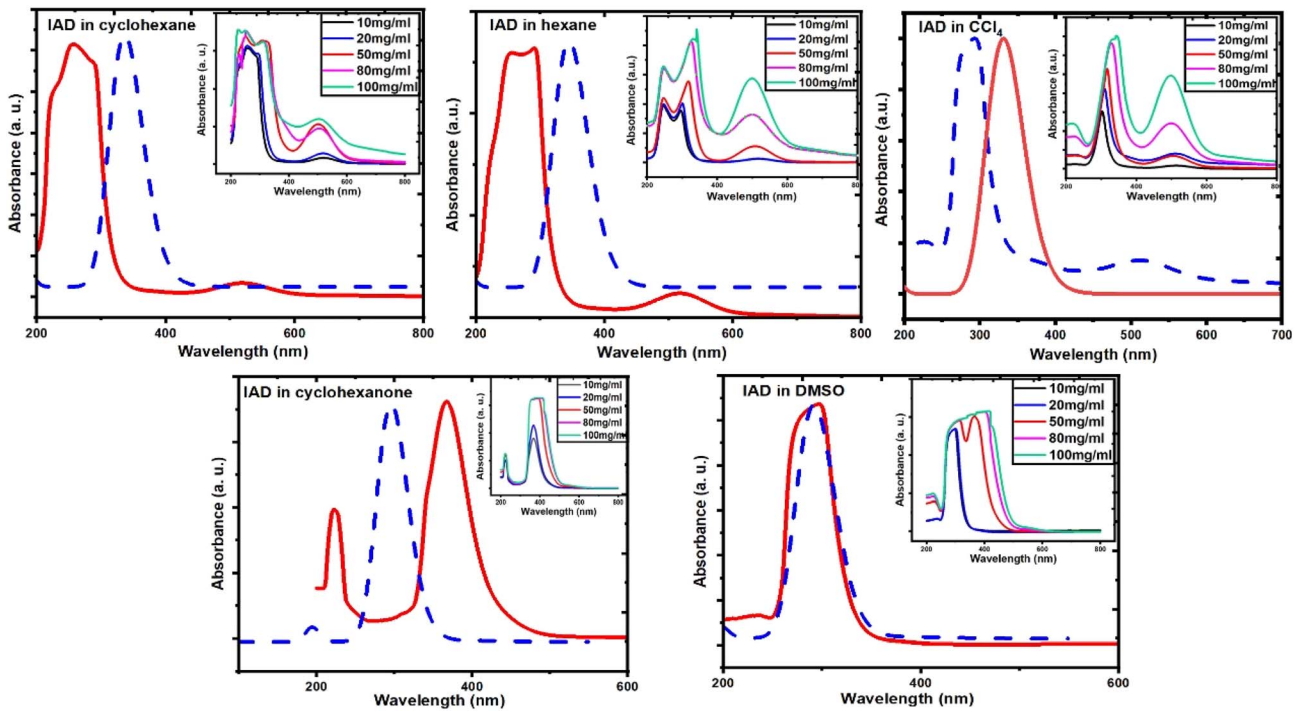

Fig. 4 Comparison of computed (dotted line) and experimental (solid line) IAD absorption spectra and concentration effects for all solvents.

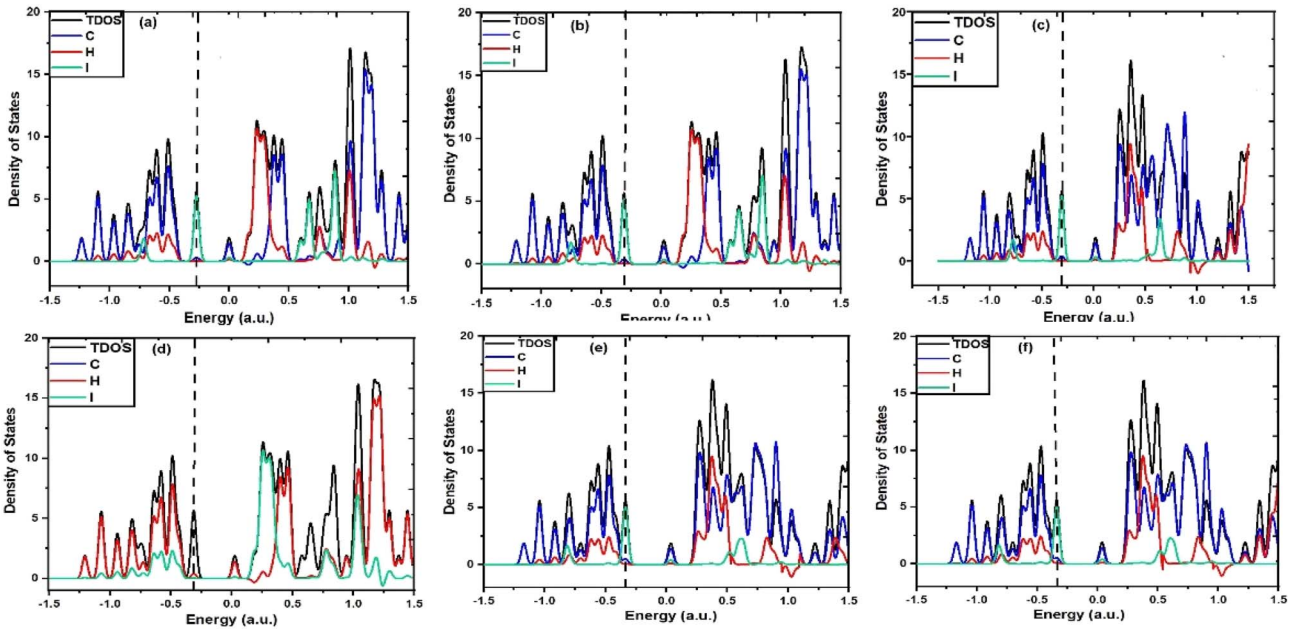

Fig. 5 TDOS and PDOS spectra of (a) IAD in the gas phase, (b) IAD in cyclohexane, (c) IAD in hexane, (d) IAD in CCL_4, (e) IAD in cyclohexanone and (f) IAD in DMSO.

to the exclusion of temperature, vibronic effects, and limitations of the theoretical model.

Solvent effect through computational analysis

To acquire a qualitative understanding of the measured solvent-induced shift in the electronic absorption, solvent influences were studied computationally by means of implicit solvation with various solvent dielectric continuums. According to this, when IAD encounters different solvent media, electron density distribution is highly influenced by the charge distribution provided by the dielectric medium with specific values of the dielectric constant for each solvation, which causes the change in the electronic absorbance. In particular, the electron density of the states experiences an energy shift and change in the occupancy. This was found to be more in polar solvents because the bonding energies of C–C bonds are sensitive to the substituents and environments, thus affecting the σ to σ* transition and it also causes significant influence on the n to σ* transition. In addition to this, partial density of states (PDOS) and total density of states (TDOS) were obtained using the Multiwfn 3.8 software,[42] as shown in Fig. 5. PDOS suggests that all the atoms are highly affected by the solvent polarity, this in turn causes substantial influence on the TDOS of IAD. The density of states for both polar and nonpolar solvents is affected, which alters the Fermi energies for both polar and nonpolar solvation.

With a maximum probable percentage of electron densities, natural bonding orbital (NBO) analysis provides a natural tenable Lewis structure of the wavefunction, which in turn provides information on the filled and virtual orbitals.[43,44] Each

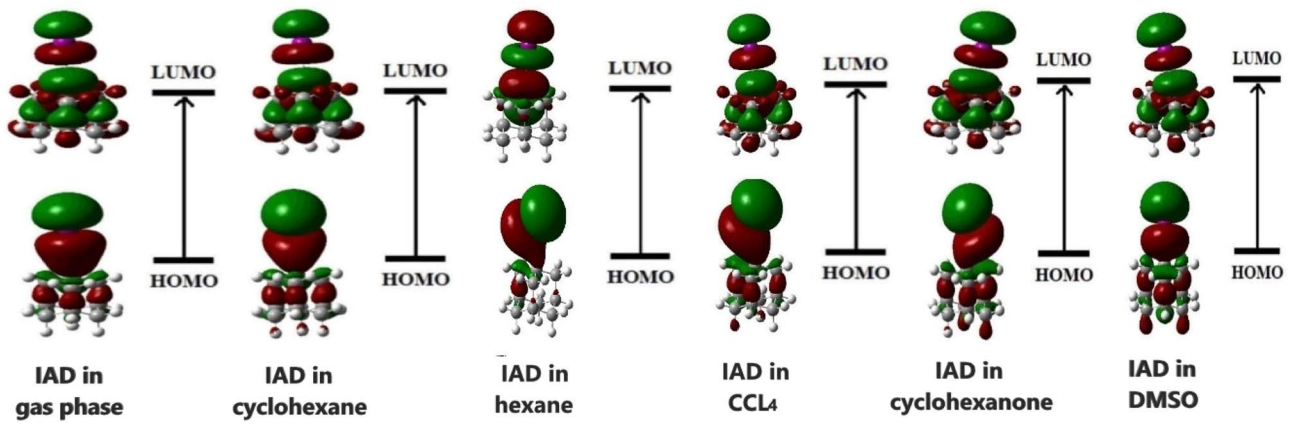

Fig. 6 Frontier molecular orbitals of IAD in different solvent media.

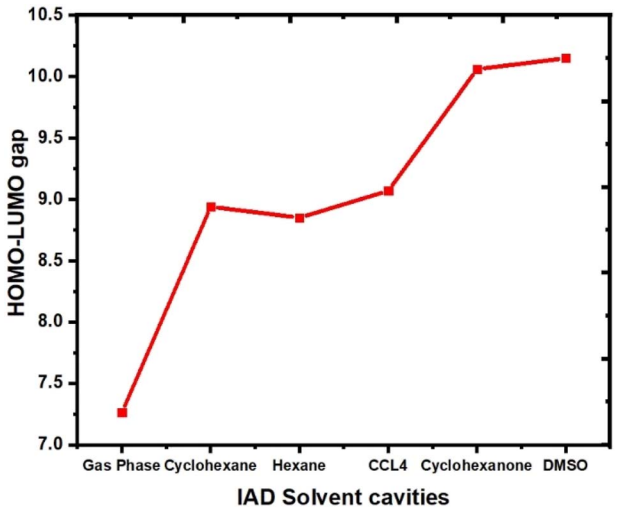

Fig. 7 The computed HOMO–LUMO gap for different solvent continuums is shown here.

donor and acceptor interaction is calculated from the second order perturbation interaction energy $E^{(2)}$, which are evaluated using the equation

$$E^{(2)} = \Delta E_{i,j} = q_i \frac{F_{(i,j)}^2}{\varepsilon_j - \varepsilon_i} \quad (2)$$

where q_i denotes donor orbital occupancy, ε_i and ε_j represents orbital energies, and $F(i,j)$ represents off-diagonal NBO Fock matrix elements.[43–45] Bonding orbital analysis showed variation in the orbital occupancies of IAD from one solvent medium to another. In polar solvents, large dipole moments of the solvents significantly alter the Rydberg and valence orbital occupancies, which are majorly responsible for n to σ* transitions. The influence of the solvent interaction on antibonding orbitals showed the variation of valence and Rydberg orbitals for the polar solvents, which is listed in Table 2. It also explains the vital role of solvent polarity on the orbitals and their occupancies.

The HOMO and LUMO of the molecules play a vital role in the chemical reactivity and stability of the molecular system.[37] The ability of a molecule to donate or accept an electron determines the electron densities of HOMO and LUMO in both ground and excited states. In the excited state, both HOMOs and LUMOs at the gas phase are localized over the entire molecular surface of IAD. In all the non-polar solvent continuum, electron densities are not significantly altered. In polar media, with respect to the polarity, HOMOs are more localized on the molecular surface, as shown in Fig. 6. This evidence of solvent-induced stabilization and notable changes in the electron densities of HOMOs and LUMOs results in the red and blue shifts in absorption due to major changes in HOMO–LUMO energies.[1,2] As a result of this, the HOMO–LUMO gap increases when the polarity of the solvent continuum increases, which is shown in Fig. 7.

The HOMO–LUMO energies of IAD are high in polar media and low in nonpolar media, and the electron densities of the HOMO and LUMO orbitals are depicted in Fig. 6. To obtain a clear insight into the active electrophilic and nucleophilic sites of IAD in different solvent media, the molecular electrostatic potential (MEP) was computed. Different colors in the reactivity maps of the MEP represented different values of the electrostatic potential (Table 3). The electron-rich region

Table 2 Summary of the computed natural population and bonding orbital analysis

Solvents	Core	Valence Lewis	Total Lewis	Valence non-Lewis	Rydberg non-Lewis	Total non-Lewis
IAD in gas phase	65.98764	61.41606	127.40370	0.48787	0.10843	0.59630
IAD in cyclohexane	65.98735	61.44055	127.42791	0.46493	0.10716	0.57209
IAD in hexane	65.98738	61.43830	127.42568	0.46708	0.10724	0.57432
IAD in CCL_4	65.98732	61.44211	127.42943	0.46346	0.10711	0.57057
IAD in cyclohexanone	65.99256	61.20936	127.20192	0.62171	0.17637	0.79808
IAD in DMSO	65.99256	61.20953	127.20209	0.62141	0.17651	0.79791

Table 3 Depiction of the molecular electrostatic potential (MEP) of IAD in different solvent media

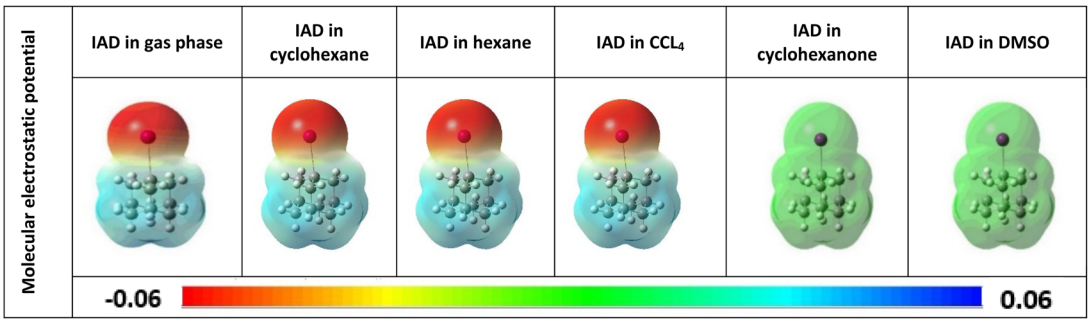

around iodine was identified as a suitable site for nucleophilic attack in the gas phase and nonpolar media, which is represented in red color. Regions suitable for electrophilic attack and zero electrostatic potentials are represented in blue and green color. The high polarity possessed by DMSO and cyclohexanone neutralizes the electrostatic potential around the iodine atom in both ground and excited states. This justified the measured blue shifts in the absorption of the polar solvents. A positive potential (σ-hole) was found in the gaseous state[46] and in all non-polar solvation media, which were unaffected by the influence of the solvent charge distribution. Due to the neutralization of the polar solvents, a σ-hole is not generated in the electrostatic potential map. Variation in the surface maxima and minima also depicts the influence of the solvent on the charge distribution of all the dielectric continuum.

Conclusions

We demonstrated significant solvatochromatic shifts in the measured absorption spectra of IAD in both polar and non-polar solvents, which is well supported by the computed results, such as HOMO and LUMO energies, electron density distribution, electrostatic potentials, and bonding orbital analysis from a molecular perspective. In this study, we found that polar solvents with relatively large dielectric constants strongly influence the electronic structure of IAD. Correspondingly, nonpolar solvents with small dielectric constant also exhibit a notable influence. A significant color change obtained for the polar solvents also supports these claims. This study elaborates on the crucial role of charge distributions provided by each solvent in determining various optical and electronic properties of the molecular system. Our attempt to expose the solvent effects was successful with experimental measurements and validated the computational calculations.

Author contributions

The conceptualization of this work was made by JH and MUM. Data collection and analysis were performed by AR. Writing and editing were performed by AR, JH, and MUM.

Conflicts of interest

There are no conflicts to declare.

Acknowledgements

The authors acknowledge the financial support provided by DST-SERB through Grant No. EMR/2016/005575 and SPG/2021/002905.

References

1 G. A. Mansoori, Diamondoid molecules, *Adv. Chem. Phys.*, 2007, **136**, 207–258.
2 F. Yang, *et al.*, Effects of molecular geometry on the properties of compressed diamondoid crystals, *J. Phys. Chem. Lett.*, 2016, **7**(22), 4641–4647.
3 O. Pirali, *et al.*, Rotationally resolved infrared spectroscopy of adamantane, *J. Chem. Phys.*, 2012, **136**(2), 024310.
4 F. Marsusi and K. Mirabbaszadeh, Altering the electronic properties of diamondoids through encapsulating small particles, *J. Phys.: Condens. Matter*, 2009, **21**(21), 215303.
5 B. Adhikari and M. Fyta, Towards double-functionalized small diamondoids: selective electronic band-gap tuning, *Nanotechnology*, 2014, **26**(3), 035701.
6 L. Wanka, K. Iqbal and P. R. Schreiner, The lipophilic bullet hits the targets: medicinal chemistry of adamantane derivatives, *Chem. Rev.*, 2013, **113**(5), 3516–3604.
7 H. Nasrallah and J.-C. Hierso, Porous materials based on 3-dimensional Td-directing functionalized adamantane scaffolds and applied as recyclable catalysts, *Chem. Mater.*, 2018, **31**(3), 619–642.
8 M. A. Gunawan, *et al.*, Diamondoids: functionalization and subsequent applications of perfectly defined molecular cage hydrocarbons, *New J. Chem.*, 2014, **38**(1), 28–41.
9 H. E. Ungnade, The effect of solvents on the absorption spectra of aromatic compounds, *J. Am. Chem. Soc.*, 1953, **75**(2), 432–434.
10 E. Papajak, *et al.*, Perspectives on basis sets beautiful: seasonal plantings of diffuse basis functions, *J. Chem. Theory Comput.*, 2011, **7**(10), 3027–3034.
11 C. D. Sherrill, An introduction to configuration interaction theory, *School of Chemistry and Biochemistry*, Georgia Institute of Technology, 1995.
12 S. N. Datta, A Coupled Cluster Theory Based on Quantum Electrodynamics, *arXiv*, 2019, preprint, arXiv:1904.11956.
13 J. B. Foresman, *et al.*, Toward a systematic molecular orbital theory for excited states, *J. Phys. Chem.*, 1992, **96**(1), 135–149.
14 I. Y. Zhang and A. Grüneis, Coupled cluster theory in materials science, *Front. Mater.*, 2019, **6**, 123.
15 J. J. Goings, *et al.*, Assessment of low-scaling approximations to the equation of motion coupled-cluster singles and doubles equations, *J. Chem. Phys.*, 2014, **141**(16), 164116.
16 Y. Ohtsuka, *et al.*, Active-space symmetry-adapted-cluster configuration-interaction and equation-of-motion coupled-cluster methods for high accuracy calculations of potential energy surfaces of radicals, *J. Chem. Phys.*, 2007, **126**(16), 164111.
17 A. B. Sannigrahi and S. D. Peyerimhoff, Extended Gaussian basis sets for iodine and their preliminary applications in abinitio configuration interaction calculations, *J. Chem. Phys.*, 1990, **93**(4), 2956–2957.
18 J. F. Stanton and R. J. Bartlett, The equation of motion coupled-cluster method. A systematic biorthogonal approach to molecular excitation energies, transition probabilities, and excited state properties, *J. Chem. Phys.*, 1993, **98**(9), 7029–7039.
19 A. Asthana, J. Liu and L. Cheng, Exact two-component equation-of-motion coupled-cluster singles and doubles method using atomic mean-field spin-orbit integrals, *J. Chem. Phys.*, 2019, **150**(7), 074102.

20 M. J. Frisch, G. W. Trucks, H. B. Schlegel, G. E. Scuseria, M. A. Robb, J. R. Cheeseman, G. Scalmani, V. Barone, G. A. Petersson, H. Nakatsuji, X. Li, M. Caricato, A. V. Marenich, J. Bloino, B. G. Janesko, R. Gomperts, B. Mennucci, H. P. Hratchian, J. V. Ortiz, A. F. Izmaylov, J. L. Sonnenberg, D. Williams-Young, F. Ding, F. Lipparini, F. Egidi, J. Goings, B. Peng, A. Petrone, T. Henderson, D. Ranasinghe, V. G. Zakrzewski, J. Gao, N. Rega, G. Zheng, W. Liang, M. Hada, M. Ehara, K. Toyota, R. Fukuda, J. Hasegawa, M. Ishida, T. Nakajima, Y. Honda, O. Kitao, H. Nakai, T. Vreven, K. Throssell, J. A. Montgomery Jr, J. E. Peralta, F. Ogliaro, M. J. Bearpark, J. J. Heyd, E. N. Brothers, K. N. Kudin, V. N. Staroverov, T. A. Keith, R. Kobayashi, J. Normand, K. Raghavachari, A. P. Rendell, J. C. Burant, S. S. Iyengar, J. Tomasi, M. Cossi, J. M. Millam, M. Klene, C. Adamo, R. Cammi, J. W. Ochterski, R. L. Martin, K. Morokuma, O. Farkas, J. B. Foresman and D. J. Fox, *Gaussian 16, Revision B.01*, Gaussian, Inc., Wallingford CT, 2016.

21 D. Roy, T. A. Keith and J. M. Millam, *GaussView, Version 6*, Semichem Inc., Shawnee Mission, KS, 2016.

22 A. B. Sannigrahi and S. D. Peyerimhoff, Extended Gaussian basis sets for iodine and their preliminary applications in abinitio configuration interaction calculations, *J. Chem. Phys.*, 1990, **93**(4), 2956–2957.

23 D. Feller, *et al.*, Performance of coupled cluster theory in thermochemical calculations of small halogenated compounds, *J. Chem. Phys.*, 2003, **118**(8), 3510–3522.

24 K. Sayin and D. Karakaş, Method and basis set investigation for trans-platinum (II)oxime complex, *Cumhuriyet Science Journal*, 2015, **36**(2), 1–10.

25 L. Li, *et al.*, Theoretical Studies on Structures, Properties and Dominant Debromination Pathways for Selected Polybrominated Diphenyl Ethers, *Int. J. Mol. Sci.*, 2016, **17**(6), 927.

26 J. Li, C. J. Cramer and D. G. Truhlar, MIDI! basis set for silicon, bromine, and iodine, *Theor. Chem. Acc.*, 1998, **99**(3), 192–196.

27 R. E. Easton, *et al.*, The MIDI! basis set for quantum mechanical calculations of molecular geometries and partial charges, *Theor. Chim. Acta*, 1996, **93**(5), 281–301.

28 A. V. Marenich, C. J. Cramer and D. G. Truhlar, Universal solvation model based on solute electron density and on a continuum model of the solvent defined by the bulk dielectric constant and atomic surface tensions, *J. Phys. Chem. B*, 2009, **113**(18), 6378–6396.

29 E. L. M. Miguel, *et al.*, How accurate is the SMD model for predicting free energy barriers for nucleophilic substitution reactions in polar protic and dipolar aprotic solvents?, *J. Braz. Chem. Soc.*, 2016, **27**(11), 2055–2061.

30 M. Reta, C. Rosa and J. J. Silber, Kamlet–Taft's solvatochromic parameters for nonaqueous binary mixtures between n-hexane and 2-propanol, tetrahydrofurane, and ethyl acetate, *J. Solution Chem.*, 2001, **30**(3), 237–252.

31 B. U. Emenike, *et al.*, Quantitative model for rationalizing solvent effect in noncovalent CH–Aryl interactions, *Chem. Sci.*, 2016, **7**(2), 1401–1407.

32 K. M. Solntsev, D. Huppert and A. Noam, Photochemistry of "super"-photoacids. Solvent effects, *J. Phys. Chem. A*, 1999, **103**(35), 6984–6997.

33 T. Islam, *et al.*, Kamlet Taft Parameters: A Tool to Alternate the Usage of Hazardous solvent in Pharmaceutical and Chemical Manufacturing/Synthesis-A Gateway towards Green Technology, *Anal. Chem. Lett.*, 2020, **10**(5), 550–561.

34 A. Eilmes, Solvatochromic probe in molecular solvents: implicit versus explicit solvent model, *Theor. Chem. Acc.*, 2014, **133**(9), 1–13.

35 T.-J. Bi, *et al.*, Solvent effects on excitation energies obtained using the state-specific TD-DFT method with a polarizable continuum model based on constrained equilibrium thermodynamics, *Phys. Chem. Chem. Phys.*, 2017, **19**(48), 32242–32252.

36 M. Yoosefian and N. Etminan, The role of solvent polarity in the electronic properties, stability and reactivity trend of a tryptophane/Pd doped SWCNT novel nanobiosensor from polar protic to non-polar solvents, *RSC Adv.*, 2016, **6**(69), 64818–64825.

37 H. C. Georg, K. Coutinho and S. Canuto, Solvent effects on the UV-visible absorption spectrum of benzophenone in water: A combined Monte Carlo quantum mechanics study including solute polarization, *J. Chem. Phys.*, 2007, **126**(3), 034507.

38 W. Kemp, *Organic Spectroscopy*, Bloomsbury Publishing, 2017.

39 E. Pretsch, *et al. Structure Determination of Organic Compounds*, Springer-Verlag, Berlin, 2000.

40 N. Mora-Diez, L. A. Montero and J. Fabian, Molecular orbital modeling of solvent effects on excited states of organic molecules, *J. Mol. Struct.: THEOCHEM*, 1998, **453**(1–3), 49–57.

41 A. Julià-López, *et al.*, Solid materials with tunable reverse photochromism, *ACS Appl. Mater. Interfaces*, 2019, **11**(12), 11884–11892.

42 T. Lu and F. Chen, Multiwfn: a multifunctional wavefunction analyzer, *J. Comput. Chem.*, 2012, **33**(5), 580–592.

43 A. E. Reed, L. A. Curtiss and W. Frank, Intermolecular interactions from a natural bond orbital, donor-acceptor viewpoint, *Chem. Rev.*, 1988, **88**(6), 899–926.

44 A. J. Pounds, *Valency and Bonding: A Natural Bond Orbital Donor–Acceptor Perspective, Frank (Weinhold and Clark Landis)*, 2007, p. 43.

45 F. Weinhold and E. D. Glendening, Comment on "natural Bond Orbitals and the Nature of the Hydrogen Bond", *J. Phys. Chem. A*, 2018, **122**(2), 724–732.

46 R. Aravindhan, M. Ummal Momeen and J. Hu, Halogenation effects on the bridgehead position of the adamantane molecule, *Chem. Phys. Lett.*, 2023, 140746.